

Topologically Protected Magnetic Helix for All-Spin-Based Applications

E. Y. Vedmedenko* and D. Altwein

University of Hamburg, Institute for Applied Physics, Jungiusstrasse 11a, 20355 Hamburg, Germany
(Received 11 July 2013; revised manuscript received 14 November 2013; published 10 January 2014)

The recent years have witnessed an emergence of the field of all-spin-based devices without any flow of charge. An ultimate goal of this scientific direction is the realization of the full spectrum of spin-based networks as in modern electronics. The concept of energy-storing elements, indispensable for those networks, are so far lacking. Analyzing analytically the size dependent properties of magnetic chains that are coupled via either exchange or long-range dipolar or Ruderman-Kittel-Kasuya-Yosida interactions, we discover a particularly simple law: magnetic configurations corresponding to helices with integer number of twists, which are commensurate with the chain's length, are energetically stable. This finding, supported by simulations and an experimentally benchmarked model, agrees with the study [R. Skomski *et al.*, *J. Appl. Phys.* **111**, 07E116 (2012)] showing that boundaries can topologically stabilize structures that are not stable otherwise. On that basis, an energy-storing element that uses spin at every stage of its operation is proposed.

DOI: 10.1103/PhysRevLett.112.017206

PACS numbers: 75.25.-j, 75.10.Hk, 75.40.Mg, 75.45.+j

A challenge for solid state physics at the nanoscale is to develop energetically efficient information and communication technologies. While spintronics, spin caloritronics, and magnonics focus on the interaction of spins with charges, heat currents, or external fields, the most recent strategy is to create devices that do not require the spin to charge conversion but that use the spin degree of freedom only to store and process information [1,3,4]. This idea is very appealing because of the variety of systems in which the micro- and nanoscopic magnetic dipoles with different anisotropy axes can now be artificially produced. The list includes atomic spin ensembles [2,3], magnetic nanoarrays [4–8], structured multilayers and superlattices [9,10], colloids [11], and molecular systems [12,13]. In order to transmit and process information without electric currents or external fields, intrinsic interactions are needed. The most ubiquitous in different kinds of magnetic system interactions are the direct and indirect [e.g., Ruderman-Kittel-Kasuya-Yosida (RKKY)] exchanges and the dipolar coupling. Short, antiferromagnetically coupled via RKKY or dipolar interaction chains (spin leads) have already been utilized to transmit the information of the state of an “input” ferromagnetic dot to the “gate” dot [1,9]. It has also been realized that the detailed structure of those antiferromagnetic (AFM) states depends on the chain length [14]. For such nanosized systems, however, there has been up to now no clear understanding of how the competition between the finite length of those chains and the order of interactions manifests itself in time-dependent magnetic order [14]. Especially intriguing is the aspect elaborated in Ref. [15], showing that boundary conditions might induce topologically protected excitations. Clearly, this lack of knowledge hampers further development of the all-spin-based information technology.

In this Letter, studying theoretically the size dependence of magnetic order in chains with exchange, RKKY, and

dipolar interactions, we discover a particularly simple law: magnetic configurations corresponding to the modulated helices with integer number of twists, which are commensurate with the chain's length, are topologically stable and correspond to local energy minima separated by energy maxima. This finding explains the stability of spin helices arising intrinsically in one dimensional systems [16–18].

We confirm these results using Monte Carlo (MC) and Landau-Lifshitz-Gilbert spin dynamics (SD) simulations and a magnetomechanical model. We also demonstrate that a chain can be forced towards one of the topologically stable states by the rotation of end spins. By further rotation, the helix can be wound up towards higher energy levels and pinned in this stable state to store energy. Unpinning this spin at a later time leads to release of the stored energy, which can be used to perform work or transfer information. The proposed device can be realized in structured multilayers [9,10], chains of nanoparticles or molecules [12,13], nanoarrays [8], and atomic chains [1].

The starting point of our calculations is a linear (along the x axis) chain of N dipoles coupled by either exchange or RKKY or dipolar interaction and possessing a uniaxial (easy axis or easy plane) anisotropy K arising due to the magneto-crystalline anisotropy, particle shape, or higher-order multipolar contributions. Here we describe results for the most complicated dipolar coupling. However, they can be straightforwardly adopted to the RKKY or exchange interactions:

$$H = D \sum_{ij} \left(\frac{\mathbf{S}_i \cdot \mathbf{S}_j}{r_{ij}^3} - 3 \frac{(\mathbf{S}_i \cdot \mathbf{r}_{ij})(\mathbf{S}_j \cdot \mathbf{r}_{ij})}{r_{ij}^5} \right) - K \sum_i (\mathbf{S}_i^x)^2, \quad (1)$$

where \mathbf{S}_i is a three-dimensional unit vector and \mathbf{r}_{ij} denotes the distance vector between moments i and j . All information

about the saturation magnetization M_s of a particle is, as usual, hidden in the interaction constant $D = \mu_0 M_s^2/2$. First, we look for the exact total number of critical points of Hamiltonian (1) solving the set of equations $\vec{\nabla} \sum_{i,j}^N H = \vec{0}$ as explained in SI1 in the Supplemental Material [21]. We reveal 3×2^N stationary points (minima, maxima, or saddle points) related to noncollinear solutions, and the question is what the magnetic configurations corresponding to these metastable states look like.

To answer this question analytically we utilize the method used for construction of spin-density waves. The magnetic structure is regarded as a superposition of spirals in the 2D Brillouin zone under the requirement of the constant magnetic moment at all sites. The energy of the constructed structure is then analyzed. The spin spirals can be described via vectors δ and q in the form (i) $\mathbf{S}(r) = \mathbf{S}[\sin(\delta r) \cos(qr), \sin(\delta r) \sin(qr), \cos(\delta r)]$ or (ii) $\mathbf{S}(r) = \mathbf{S}[\sin(\delta r), \cos(\delta r) \sin(qr), \cos(\delta r) \cos(qr)]$. For $q = 0$ and $\mathbf{r} \parallel \mathbf{Ox}$, for example, (i) gives a spin spiral $\mathbf{S}(x) = \mathbf{S}[\sin(\delta x), 0, \cos(\delta x)]$ in the xz plane. The energy of this spin configuration as a function of δ is plotted as a dashed line in Fig. 1(a). It is seen that the energy is minimal ($E_{\min 1}$) at $\delta = \pi$, i.e., corresponds to the AFM alignment of neighboring spins and is known as the ground state of a chain with easy xz plane [see Fig. 1(c)]. There is only one minimum in this case, and the envelope lines of the AFM structure Fig. 1(c) are straight. If, however, (δ, q) differ from these special values, the energy spectrum changes dramatically: it adopts many local energy minima and maxima, in good agreement with our analytical analysis. The contour plot of the energy $E(\delta, q)$ for a chain of $N = 10$ dipoles is shown in Fig. 1(b). Several cross sections of this two-dimensional energy surface for different K are shown in Fig. 1(a). Fascinatingly, the minima occur for all $\{q, \delta\} = \{\pm(n\pi/N), \pi \pm (m\pi/N)\}$ for $K < -2.3D$ and $\{q, \delta\} = \{\pm(n\pi/N), \pi \pm (\pi/2N) + (m\pi/N)\}$ for $K > 2.3D$ with integer $m \in [0, N]$ and $n \in [0, N]$. In other words, the energy spectrum becomes discrete and the energy gaps become size dependent; i.e., we observe all components of quantum confinement. The deepest minima, i.e., stablest energy levels, correspond to magnetic helices (MH) with integer number of turns along the chain, as shown in Fig. 1(c), and can be uniquely described using quantum numbers m and n defining wave vectors δ and q , which are commensurate to the chain length. The number of helix turns is given by the smaller wave vector. For example, if $\delta \geq \pi$, then $q = \pi/N$ corresponds to one helix turn of the entire chain.

To explore complete configurational space beyond the two-wave-vectors approximation, MC and SD simulations have been performed. Additionally, a magnetomechanical model presented in Fig. 2 and described in [21] has been constructed. While the MC procedure has been developed to describe the equilibrium properties of many-body systems, the SD gives an exact dynamical path from one

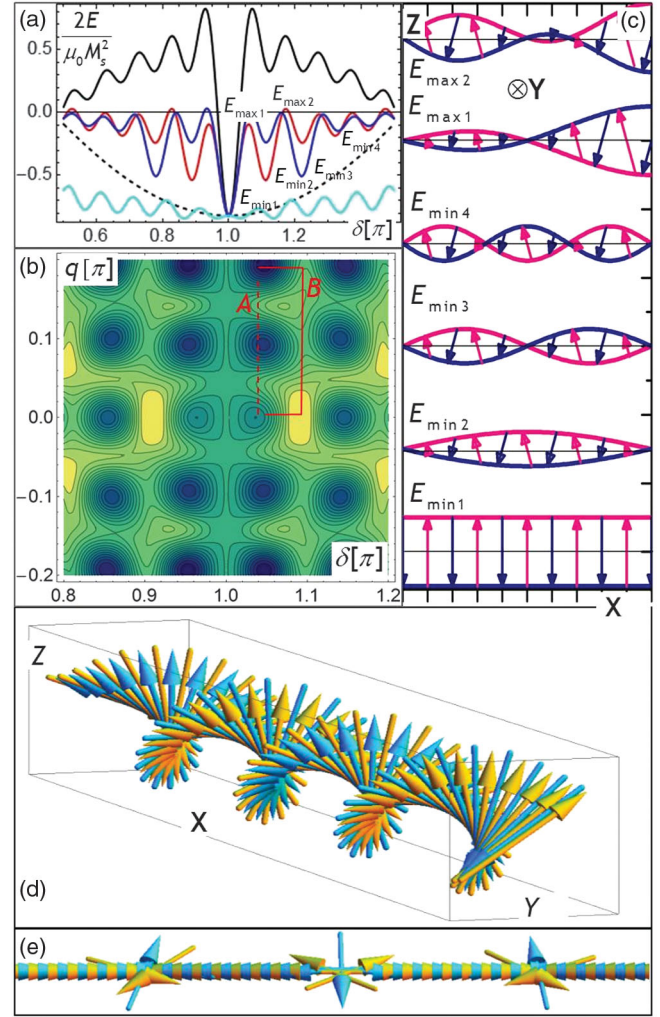


FIG. 1. (a),(b) One- and two-dimensional representation of the energy of modulated helices in a dipolar chain consisting of 10 moments as a function of δ and q . (c) $S_z(r)$ for several energy levels. The thick lines in (c) show the envelope lines of double helices corresponding to the magnetic moments (arrows) in two sublattices. The dashed parabola in (a) corresponds to the energy of the harmonic spiral $\mathbf{S}(x) = \mathbf{S}(\sin \delta x, 0, \cos \delta x)$; the black, red, and blue curves correspond to $E(\delta)$ of modulated helices with $K = 0$ and $q = 0$, $q = \pi/N$, and $q = 2\pi/N$, respectively, while the cyan line shows $E(\delta)$ for $q = \pi/N$ and $K = 2.5D$. The energy scale in (b) goes linearly from $-0.8D$ (blue) to $+0.8D$ (yellow). (d) Three-dimensional representation of an intermediate helix state found in the SD simulations for $N = 81$ (video SI2 [21]) for $K = 1.23\mu_0 M_s^2$ at $T < 1 K$. (e) End configuration of SD simulations for $K = 0$ and starting configuration identical to (d).

configuration to another. The details of the numerical procedure are described in [19–21]. According to the MC analysis, the stable equilibrium configuration of a dipolar chain of length N for $kT > 0.1D$ and $-1.2D < K < 2D$ indeed corresponds to $E_{\min 2}$ in Fig. 1(c), i.e., to $(q, \delta) = (\pi/N, \pi \pm (\pi/N))$. Only at lower temperatures or higher anisotropy the ground AFM state can be achieved. Our SD simulations demonstrate that the exact dynamical

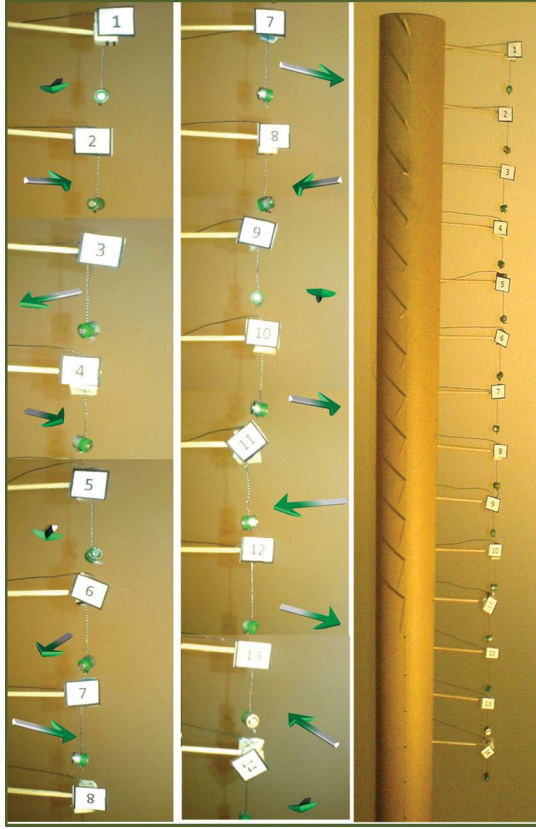


FIG. 2. Magnetomechanical model [21]. The magnets do not contain any connecting wire. They are hanging each on its own soft, nonmagnetic filament and coupled via magnetostatics only. The hole is larger than the diameter of the filament and magnets may rotate without screwing it. Left: Stable spin helix with modulation vector $q = (3/2)(\pi/14)$. Right: General view of the model. Silver and green colors represent the north and the south poles, respectively.

path towards the global energy minimum strongly depends on the starting configuration and passes through several energy MH states as predicted above. Starting with the $S\{\sin[(\pi + (\pi/N))x], \cos[(\pi + (\pi/N))x], 0\}$ state, e.g., one ends up with a half-turn helix for anisotropy comparable with the dipolar energy. Another example of dynamical relaxation is recorded in video SI2 in the Supplemental Material [21], while one of intermediate configurations is shown in Fig. 1(d). Even for $K = 0$ the system often freezes in modulated structure, as shown in Fig. 1(e). In accordance with the simulations, the most probable stable states of the experimental chain established after mechanical agitation were spin spirals with π or $\pi/2$ twist. In addition to the easy-plane rotation of magnetization, a systematic modulation of the easy-axis component was also clearly observable. The less probable, but still stable, spiral with $q = 3\pi/2N$ configuration is documented in Fig. 2.

The reasons for the stability of MHs are as follows: (i) the internal fields in these structures coincide with the orientation of dipoles, and (ii) those states cannot be

transformed into the ground state by continuous deformation; i.e., they are topologically stable. Hence, if one fixes the ends of a chain, the helical structure will remain at the local energy minimum. Next, we want to use this property to achieve different (δ, q) states artificially. To do so, we propose to rotate magnetization of one of the terminal dipoles introducing energy into the chain. The consequences of this procedure are documented in MC simulations (Fig. 3), SD simulations (videos SI3,4,6 [21]), and magnetomechanical model (video SI5 [21]).

The Monte Carlo simulations have been performed for chains of length $N = 70a$. The equilibrium winding-up process is shown in Fig. 3(a). Initially, the slow annealing procedure has been applied. At the end of this relaxation, at $kT = 0.05D$, the chain has adopted the MH state with $q = \pi/N$; i.e., the entire chain acquired half of a modulation period. This state was taken as the starting configuration for the winding-up process. Next, the first spin has been rotated with the velocity $(\pi/2)/(2 \times 10^5 \text{ MCS})$, because our analysis showed that the period of $2 \times 10^5 \text{ MCS}$ was long enough to achieve a new equilibrium state. After nine subsequent rotations, which are illustrated Fig. 3(a), the chain arrived at the stable $q = 5\pi/2N$ helix. The other end of the chain remained free. In Fig. 3(b) the time dependence of the z component of magnetization for the first and the last spins is monitored. One sees that the rotation of the last spin is somewhat delayed comparably to the rotation of the first spin because of the system's retarding in the stable energy levels. Another interesting observation concerns the propagation velocity of a knot in the spiral. The velocity of propagation

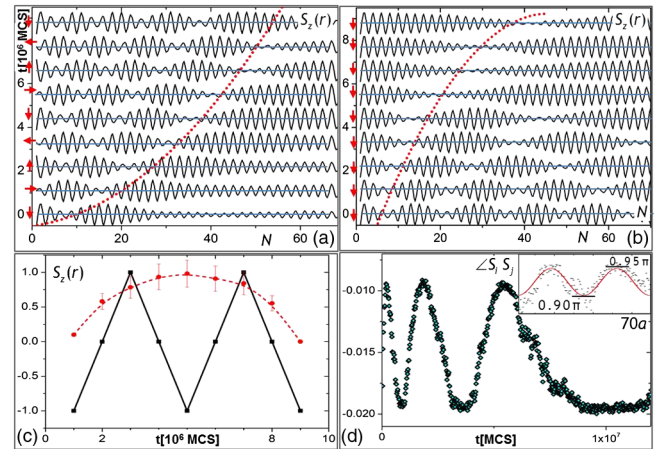


FIG. 3 (color online). MC simulations of a linear chain of 70 dipoles with $K = 1.23\mu_0 M_s^2$ at $kT < 1 \text{ K}$. (a) Winding up of the spiral. Each snapshot of $S_z(r)$ corresponds to a relaxed state. The far-left moment (red) has been rotated with velocity of $(\pi/2) \times 10^5 \text{ MCS}$. (b) Time dependence of the far-left (black line) and the far-right (red line) moments. (c) Release of the stored energy: the left moment is fixed downwards. (d) Nonlinear time dependence of the chain-averaged $\langle S_z \rangle$. A typical angle distribution in a relaxed helix is shown in the inset.

decreases with increasing q , as shown by dashed red line, and can be described by a function of the form $v = at^2$ with the negative acceleration a . The backward process is depicted in Figs. 3(c) and 3(d). The first spin is fixed now and the chain's relaxation is monitored. The back rotation was again decelerated, as shown in Fig. 3(d). The whole process, however, took much longer as the spiral had been released at the local energy minimum.

The MC results are in very good agreement with the SD simulations shown in video SI3,4 for dipolar coupling and SI6 for ferromagnetic exchange interaction [21]. The time scale depends on the strength of the magnetic interactions and damping parameters. For a chain made out of $35 \times 35 \times 2$ nm nanoparticles, interparticle distance 20 nm, and Gilbert damping of 0.01, the entire winding-up process of video SI3,4 [21] corresponds to milliseconds. Additionally, SD reveals new interesting aspects of the winding process. The first, evident conclusion is that the velocity of the entire process depends on the velocity of forced rotation of the first spin. The unexpected finding is that formation of each new turn of the magnetic helix is accompanied by an abrupt change in the magnetization of several dipoles in the case of dipolar interaction. Initially, the neighbors of the first dipole rotate coherently with a certain phase shift. The internal energy of the chain climbs thereby towards a local energy maximum (e.g., $E_{\max 1}$ in Fig. 1). When the rotation angle approaches a critical value, the local maximum is achieved, and an abrupt change in the orientations of dipoles happens as the system falls down into the next stable state corresponding to two turns of the helix (see video SI3 [21]). During this process some of the dipoles continue to rotate in the direction of forced winding up, while others rotate in the opposite direction. In our magneto-mechanical experiment, the states with larger q 's are also achieved after the magnetization jumps described above, as demonstrated in video SI5 [21]. Hence, the magnetic helix can be "clicked into place," which is different from Dzyaloshinskii-Moriya spin spirals [3] as discussed in [21]. The click into place behavior during the winding-up process exists also for $q = 0$, i.e., for $S_x = 0$. If we repeat the same procedure for a chain coupled via nearest-neighbor ferromagnetic exchange interaction with the same interaction strength and damping, the behavior is the same but no jumps occur (see video SI6 [21]), because the relaxation time of the chain becomes comparable with the angular rotation velocity. When a wound-up chain is released (video SI4 [21]), the stored energy becomes large enough to overcome several barriers.

The unusual properties of MH open several interesting perspectives in view of applications. Probably the most important one concerns the new way of energy storage. One of the oldest methods, which is still actively utilized in a number of applications, is the spring wind-up technique. An example, familiar to everyone, is a clockwork device mechanically powered by a mainspring. In this method one end of a mechanical spring is fixed, while the other is

rotated until the spring is wound up. Then the latter spring terminal is released and the stored potential energy transforms into the kinetic energy of a clock arrow, a motor, a pump, etc. A similar procedure can be applied to the MHs. By rotation of one chain's end via local fields or spin-polarized currents, the helix can be forced towards smaller periodicities and, thus, higher energy. The system can be left in this new stable configuration to store introduced energy. The stored energy can then be transformed into its mechanical or magnetic counterparts to make work as visualized in the videos in [21] and Fig. 3.

In conclusion, the results described above demonstrate that the finite magnetic chains coupled by an exchange, RKKY, or dipolar interactions possess a quantized energy spectrum depending on the chain geometry, material of elements, and the shape of the particles. This unique energy spectrum results in topologically protected configurations in the form of magnetic helices with integer number of revolutions and opens broad perspectives for future investigations concerning the dynamics of this nontrivial system and quantum effects on length scales from micrometer to a few angstrom.

Support by the DFG (SFB 668) is gratefully acknowledged.

*vedmeden@physnet.uni-hamburg.de

- [1] A. A. Khajetoorians, J. Wiebe, B. Chilian, and R. Wiesendanger, *Science* **332**, 1062 (2011).
- [2] L. Zhou, J. Wiebe, S. Lounis, E. Vedmedenko, F. Meier, S. Blügel, P. H. Dederichs, and R. Wiesendanger, *Nat. Phys.* **6**, 187 (2010).
- [3] M. Menzel, Y. Mokrousov, R. Wieser, J. E. Bickel, E. Vedmedenko, S. Blügel, S. Heinze, K. von Bergmann, A. Kubetzka, and R. Wiesendanger, *Phys. Rev. Lett.* **108**, 197204 (2012).
- [4] B. Behin-Aein, D. Datta, S. Salahuddin, and S. Datta, *Nat. Nanotechnol.* **5**, 266 (2010).
- [5] E. Mengotti, L. J. Heyderman, A. F. Rodríguez, F. Nolting, R. V. Hügli, and H.-B. Braun, *Nat. Phys.* **7**, 68 (2011).
- [6] J. P. Morgan, A. Stein, S. Langridge, and C. H. Marrows, *Nat. Phys.* **7**, 75 (2011).
- [7] A. Schumann, P. Szary, E. Y. Vedmedenko, and H. Zabel, *New J. Phys.* **14**, 035015 (2012).
- [8] M. Ewerlin, D. Demirbas, F. Brüssing, O. Petracic, A. A. Ünal, S. Valencia, F. Kronast, and H. Zabel, *Phys. Rev. Lett.* **110**, 177209 (2013).
- [9] A. Fernandez-Pacheco, D. Petit, R. Mansell, R. Lavrijsen, J. H. Lee, and R. P. Cowburn, *Phys. Rev. B* **86**, 104422 (2012).
- [10] M. van Kampen *et al.*, *J. Phys. Condens. Matter* **17**, L27 (2005).
- [11] N. Mikuszeit, L. Baraban, E. Vedmedenko, A. Erbe, P. Leiderer, and R. Wiesendanger, *Phys. Rev. B* **80**, 014402 (2009).
- [12] K. Bernot, L. Bogani, A. Caneschi, D. Gatteschi, and R. Sessoli, *J. Am. Chem. Soc.* **128**, 7947 (2006).
- [13] W. Wernsdorfer, *Nat. Mater.* **6**, 174 (2007).

- [14] A. A. Khajetoorians, J. Wiebe, B. Chilian, S. Lounis, S. Blügel, and R. Wiesendanger, *Nat. Phys.* **8**, 497 (2012).
- [15] R. Skomski *et al.*, *J. Appl. Phys.* **111**, 07E116 (2012).
- [16] S. Bedanta, E. Kentzinger, O. Petravic, W. Kleemann, U. Rücker, Th. Brückel, A. Paul, S. Cardoso, and P. P. Freitas, *Phys. Rev. B*, **74**, 054426 (2006).
- [17] B. Braunecker, P. Simon, and D. Loss, *Phys. Rev. B* **80**, 165119 (2009).
- [18] J. Klinovaja, P. Stano, A. Yazdani, and D. Loss, *Phys. Rev. Lett.* **111**, 186805 (2013).
- [19] E. Y. Vedmedenko and N. Mikuszeit, *ChemPhysChem* **9**, 1222 (2008).
- [20] U. Nowak, *Annu. Rev. Comput. Phys.* **IX**, 105 (2001).
- [21] See Supplemental Material at <http://link.aps.org/supplemental/10.1103/PhysRevLett.112.017206> for videos S11–S16.